ISBN: 978-3-95450-241-7 ISSN: 2673-5350 doi:10.18429/JACoW-IBIC2022-TU3I1

INVESTIGATING THE TRANSVERSE DYNAMICS OF ELECTRON BUNCHES IN LASER-PLASMA ACCELERATORS

A. Koehler*,[1], German Aerospace Center (DLR e.V.), Fassberg, Germany
[1]previously at Helmholtz-Zentrum Dresden – Rossendorf, Dresden, Germany

Abstract

The demonstrations of GeV electron beams and FEL radiation driven by a centimeter-scale device illustrate the tremendous progress of laser-plasma accelerators. In such applications, beam divergence and size, along with beam energy and charge, are critical parameters of electron beams. An insight on the transverse parameters and their dynamics such as beam decoherence can be obtained by diagnostics complemented by betatron radiation detectors. This talk will also provide a brief overview of recent techniques for accessing the transverse phase space.

INTRODUCTION

Relativistic electron sources represent an important tool in basic and applied sciences. The best examples are synchrotron light facilities and free-electron lasers (FELs), in which electrons produce extremely short and bright flashes of light as they pass through periodic structures. This radiation allows us to study ultrashort processes and nonequilibrium states in biology, chemistry, and materials science. However, the radiofrequency technology generally used limits the maximum electron current and thus the available radiation intensity due to its accelerating structures. Ultimately, this leads to huge, expensive accelerators that can only be made available to a small group of users. In contrast to conventional accelerators, plasma accelerators produce highly relativistic electrons of up to several GeV at much shorter acceleration lengths of only a few millimeters. Because of the high beam currents enabled by the plasma medium, they are ideally suited for driving FELs, as demonstrated recently [1, 2].

Plasma accelerators can be driven by intense laser radiation, e.g. in laser wakefield acceleration (LWFA) schematically shown in Fig. 1. In LWFA, a high-intensity laser pulse propagates through an underdense plasma of density n_e, exciting plasma waves of frequency $\omega_p = \sqrt{n_e e^2/(m_e \epsilon_0)}$. Here, e, m_e and ϵ_0 are the elementary charge, the electron mass, and the vacuum permittivity, respectively. The waves are excited by the ponderomotive force of the laser pulse, which displaces electrons from high intensity regions. At relativistic laser intensities, the electrons are completely pushed from the high intensity regions by the laser pulse. Due to their large mass, the ions remain behind and form a plasma cavity or a so-called bubble [3]. Electrons in a plasma cavity experience a longitudinal accelerating electric field and gain the energy γ. In the transverse plane, the plasma's electric and magnetic fields continuously focus

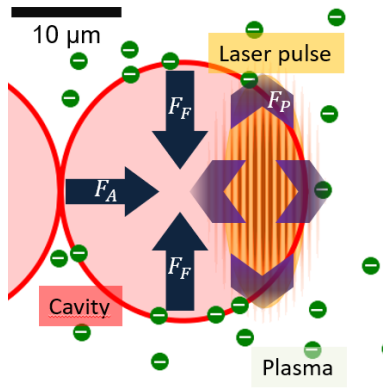

Figure 1: Schematic of LWFA. The laser pulse moves from left to right. F_P, F_F and F_A are the ponderomotive force of the laser pulse and the focusing and accelerating forces of the cavity on injected electrons, respectively.

the electrons and cause them to oscillate at the betatron frequency $\omega_\beta = \omega_p/\sqrt{2\gamma}$ and wavelength λ_β. The resulting betatron radiation enables the study of beam dynamics inside the plasma as well as it provides a broadband, ultrashort x-ray source [4].

The characteristics of betatron radiation can be compared with radiation from undulators and wigglers [5]. The dimensionless wiggler parameter for LWFA depends on the betatron radius r_β as

$$K = 2\pi\gamma\frac{r_\beta}{\lambda_\beta}. \quad (1)$$

The betatron radius is the amplitude of the electron orbit during acceleration. The betatron radiation spectrum is synchrotron-like and is described by the critical energy $E_c = 3\gamma^2 K h\omega_\beta$, where h is the Planck constant.

Typical LWFA operating at plasma densities of $1 \times 10^{19}\,\mathrm{cm}^{-3}$ possesses plasma wavelengths of 10 µm. When the accelerated electrons reach energies of about 250 MeV at typical r_β of 1 µm, then $K \approx 10$ indicates the wiggler regime and the emitted spectrum has a critical energy of about 10 keV.

The paper is structured as follows: First, a basic setup for LWFA is shown, including commonly utilized betatron diagnostics. Then, very briefly, betatron decoherence is introduced. Finally to a short summary, laser-acceleration methods of other particles are mentioned.

* Alexander.koehler@dlr.de

ISBN: 978-3-95450-241-7 ISSN: 2673-5350 doi:10.18429/JACoW-IBIC2022-TU3I1

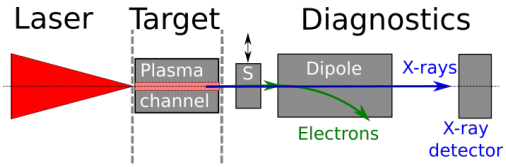

Figure 2: Schematic example of an LWFA setup. The retractable detector S can be, for example, a scintillation screen or a current transformer for the electron beam.

SETUP AND BUNCH DIAGNOSTICS

Basic Components of an LWFA Setup

As shown in Fig. 2, a typical LWFA setup consists of three components: a high-power laser system, a target, and diagnostics. The laser system, for example, delivers a pulse energy of several joules at pulse durations in the range of 100 to 30 fs [6]. To achieve high intensities, the laser pulse is focused down to spot sizes of 10s of µm on the target, that are comparable with the plasma wavelength. Jets from gas nozzles and gas-filled capillaries operated with easily ionizable gases such as helium or hydrogen can be used as targets. Both differ in adjustable plasma densities and lengths and depend on the deployed injection scheme. The highly versatile diagnostics analyze the properties of electrons that are accelerated by and copropagate with the laser pulse [7]. Charge can be detected either by fast current transformers or by charge-calibrated scintillation screens [8]. Typically, at least an electron spectrometer is utilized for obtaining an energy-resolved spectrum. The spectrometer's dipole magnet deflects the accelerated electrons on a calibrated screen.

Betatron Diagnostics

The betatron spectrum can be reconstructed by detecting single photons with a CCD X-ray camera [9]. Another method is to use dispersive elements such as crystals or powders [10]. Both detection methods have advantages and disadvantages. Single photon detection requires a sufficiently low intensity on the chip, since typically only about 1% to 5% of the detector's pixels may be hit by a photon to be able to isolate single photon events. On the other hand, only the low-energy part of the betatron spectrum can be efficiently scattered by a Bragg crystal, since the resolution at high X-ray energies is too low. Therefore, single photon detectors are placed several meters away from the source, while crystal-based detectors are typically only one meter away to collect a sufficient amount of photons. Alternatively, when space is restricted, a set of multiple foils can be assembled to pass only parts of the spectrum.

Betatron spectroscopy is a non-invasive and indirect diagnostic method. Figure 3 shows an example of a measured betatron spectrum. Single photon detectors may suffer from the high photon flux. In this case, the number of detected photons can be reduced by filter foils, which are the main source of attenuation of the red shaded area. The betatron radius can be acquired by the spectral shape. The spectrum

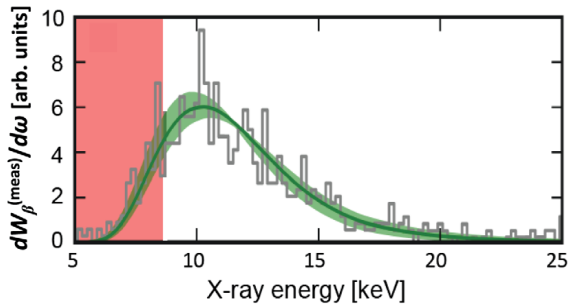

Figure 3: Example of a measured betatron spectrum with single photon detectors. The solid black histogram shows the photons counted per energy bin. The solid green line is the best fit for a betatron radius of 0.8 µm. The red shaded area is the lower detection limit due to beam line transmission and detector efficiency. From [7].

is dominated by the radiation emitted at the end of the acceleration, i.e. still in the plasma.

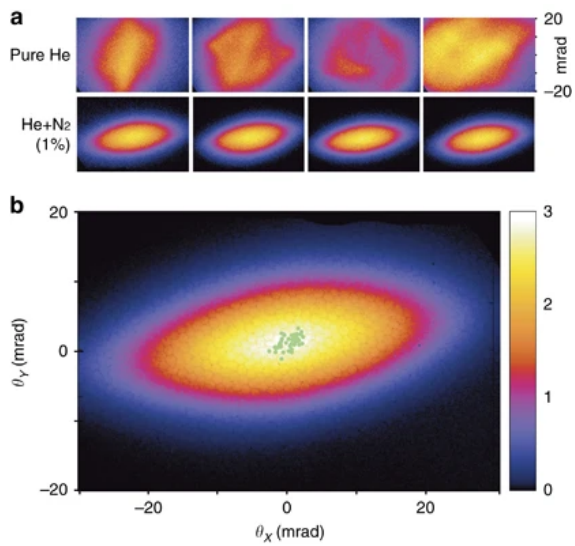

Figure 4: The typical spatial profile of betatron radiation depends on the way electrons are injected into the accelerator. (a) shows two different gas mixtures that can be used to tune the profile and thus the electron orbits. (b) is the average signal over 50 consecutive shots using He+N_2 as the gas mixture. From [11].

Beside the spectrum, the spatial profile of the radiation can provide information about the orientation of the electron orbits during acceleration [11]. Depending on the type of injection, the accelerated electrons will perform betatron oscillations in one prefered plane or in both transverse planes, resulting in elliptic or circular beam profiles, as presented in Fig. 4. The spatial profile can be detected by carefully light shielded scintillators, such as CsI or Lanex [8] that has to be protected from residual laser light and energetic electrons.

ISBN: 978-3-95450-241-7 ISSN: 2673-5350 doi:10.18429/JACoW-IBIC2022-TU3I1

Complementing Diagnostics

The high beam divergence of electrons from LWFA compared to RF-based accelerators allows short drift distances to determine the beam divergence σ_θ despite high energies. A very elegant method is to use the non-dispersive plane of a dipole magnet while the electron energy γ is detected simultaneously in the dispersive plane. Then, the beam size σ_r can be deduced from the critical energy, allowing to estimate the normalized emittance by an elaborated model [12]. For LWFA, emittances as low as 0.1 mm · mrad up to several mm mrad has been reported [7, 13].

BUNCH DECOHERENCE

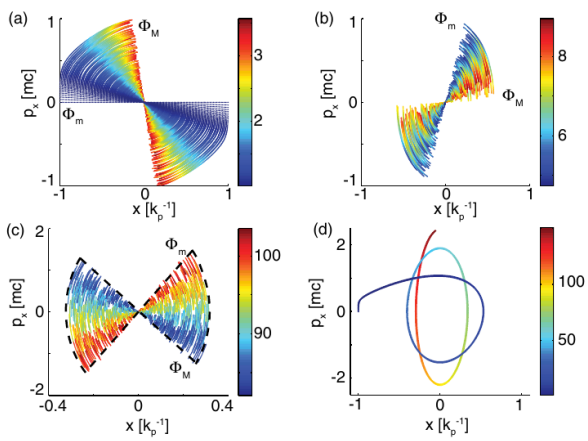

Figure 5: Transverse phase space (x, p_x) during the decoherence process. The color indicates the electron energy γ. (a)-(c) are taken at different times during acceleration. (a) is at the beginning of the acceleration ($\gamma \approx 2$), (b) is after a small energy gain ($\gamma \approx 7$), and (c) after a larger energy gain ($\gamma \approx 95$). (d) is the phase space trajectory for a single randomly selected particle. From [14].

One phenomenon that can be studied with LWFA due to the constant focusing in the plasma channel is the decoherence of the bunch [14, 15]. In the transverse phase space of location and momentum, the electron orbits describe circular paths that are traversed more slowly with progressive adiabatic acceleration. Due to the energy dependence of the betatron frequency, it happens that electron groups with different energies can twist relative to each other and also overtake each other, as shown in Fig. 5. The result is a dynamically evolving normalized emittance that can be minimized under optimal conditions.

CONCLUSION

LWFA has become a reliable source and acceleration method for relativistic electrons [16, 17]. At the same time, diagnostics that detect the beam parameters [18] or resolve the very compact plasma structures [19, 20] have also become more sophisticated. In this paper, only a small part of this could be described.

Plasma-based accelerators allow colliders and FELs to be designed much more compactly, making them accessible to a wider range of users. With the availability of inherently synchronized laser pulses, laboratories with LWFA sources also offer unique opportunities for pump-probe setups for investigation with multiple beam types (electrons, X-rays, infrared and visible laser radiation) [21].

ACKNOWLEDGEMENTS

The author would like to thank the conference organizers and the DLR for their support and for the opportunity to present an invited talk.

REFERENCES

[1] W. Wang *et al.*, "Free-electron lasing at 27 nanometres based on a laser wakefield accelerator", *Nature*, vol. 595, pp. 516–520, 2021. doi:10.1038/s41586-021-03678-x

[2] R. Pompili *et al.*, "Free-electron lasing with compact beam-driven plasma wakefield accelerator", *Nature*, vol. 605, pp. 659–662, 2022. doi:10.1038/s41586-022-04589-1

[3] A. Pukhov and J. Meyer-ter-Vehn, "Laser wake field acceleration: the highly non-linear broken-wave regime", *Appl. Phys. B: Lasers Opt.*, vol. 74, pp. 355–361, 2002. doi:10.1007/s003400200795

[4] F. Albert and A. G. R. Thomas, "Applications of laser wakefield accelerator-based light sources", *Plasma Phys. Controlled Fusion*, vol. 58, p. 103001, 2016. doi:10.1088/0741-3335/58/10/103001

[5] S. Corde *et al.*, "Femtosecond x rays from laser-plasma accelerators", *Rev. Mod. Phys.*, vol. 85, pp. 1–48, 2013. doi:10.1103/RevModPhys.85.1

[6] U. Schramm *et al.*, "First Results with the Novel Peta-Watt Laser Acceleration Facility in Dresden", in *Proc. IPAC'17*, Copenhagen, Denmark, May 2017, pp. 48–52. doi:10.18429/JACoW-IPAC2017-MOZB1

[7] M. C. Downer *et al.*, "Diagnostics for plasma-based electron accelerators", *Rev. Mod. Phys.*, vol. 90, p. 035002, 2018. doi:10.1103/RevModPhys.90.035002

[8] T. Kurz *et al.*, "Calibration and cross-laboratory implementation of scintillating screens for electron bunch charge determination", *Rev. Sci. Instrum.*, vol. 89, p. 93303, 2018. doi:10.1063/1.5041755

[9] A. Köhler *et al.*, "Single-shot betatron source size measurement from a laser-wakefield accelerator", *Nucl. Instrum. Methods Phys. Res., Sect. A*, vol. 829, p. 265, 2016. doi:10.1016/j.nima.2016.02.031

[10] M. Šmíd *et al.*, "Highly efficient angularly resolving x-ray spectrometer optimized for absorption measurements with collimated sources", *Rev. Sci. Instrum.*, vol. 88, p. 063102, 2017. doi:10.1063/1.4986464

[11] A. Doepp *et al.*, "Stable femtosecond X-rays with tunable polarization from a laser-driven accelerator", *Light Sci. Appl.*, vol. 6, p. e17086, 2017. doi:10.1038/lsa.2017.86

[12] A. Curcio *et al.*, "Trace-space reconstruction of low-emittance electron beams through betatron radiation in laser-plasma accelerators", *Phys. Rev. Accel. Beams*, vol. 20, p. 012801, 2017. doi:10.1103/PhysRevAccelBeams.20.012801

ISBN: 978-3-95450-241-7 ISSN: 2673-5350 doi:10.18429/JACoW-IBIC2022-TU3I1

[13] G. Plateau *et al.*, "Low-Emittance Electron Bunches from a Laser-Plasma Accelerator Measured using Single-Shot X-Ray Spectroscopy", *Phys. Rev. Lett.*, vol. 109, p. 64802, 2012. doi:10.1103/PhysRevLett.109.064802

[14] X. Xu *et al.*, "Phase-Space Dynamics of Ionization Injection in Plasma-Based Accelerators", *Phys. Rev. Lett.*, vol. 112, p. 035003, 2014. doi:10.1103/PhysRevLett.112.035003

[15] A. Koehler *et al.*, "Restoring betatron phase coherence in a beam-loaded laser-wakefield accelerator", *Phys. Rev. Accel. Beams*, vol. 24, p. 091302, 2021. doi:10.1103/PhysRevAccelBeams.24.091302

[16] J. Götzfried *et al.*, "Physics of High-Charge Electron Beams in Laser-Plasma Wakefields", *Phys. Rev. X*, vol. 10, p. 041015, 2020. doi:10.1103/PhysRevX.10.041015

[17] A. R. Maier *et al.*, "Decoding Sources of Energy Variability in a Laser-Plasma Accelerator", *Phys. Rev. X*, vol. 10, p. 031039, 2020. doi:10.1103/PhysRevX.10.031039

[18] A. Seidel *et al.*, "Characterizing ultralow emittance electron beams using structured light fields", *Phys. Rev. Accel. Beams*, vol. 24, p. 012803, 2021. doi:10.1103/PhysRevAccelBeams.24.012803

[19] S. Schöbel *et al.*, "Effect of driver charge on wakefield characteristics in a plasma accelerator probed by femtosecond shadowgraphy", *New J. Phys.*, vol. 24, p. 083034, 2022. doi:10.1088/1367-2630/ac87c9

[20] M. B. Schwab *et al.*, "Visualization of relativistic laser pulses in underdense plasma", *Phys. Rev. Accel. Beams*, vol. 23, p. 032801, 2020. doi:10.1103/PhysRevAccelBeams.23.032801

[21] B. Kettle *et al.*, "Single-Shot Multi-keV X-Ray Absorption Spectroscopy Using an Ultrashort Laser-Wakefield Accelerator Source", *Phys. Rev. Lett.*, vol. 123, p. 254801, 2019. doi:10.1103/PhysRevLett.123.254801